SCIENTIFIC REPORTS

OPEN

Inhibition of Beta-Amyloid Fibrillation by Luminescent Iridium(III) Complex Probes

Received: 03 March 2015
Accepted: 01 May 2015
Published: 30 September 2015

Lihua Lu[1,*], Hai-Jing Zhong[2,*], Modi Wang[1], See-Lok Ho[1], Hung-Wing Li[1], Chung-Hang Leung[2] & Dik-Lung Ma[1]

We report herein the application of kinetically inert luminescent iridium(III) complexes as dual inhibitors and probes of beta-amyloid fibrillogenesis. These iridium(III) complexes inhibited $A\beta_{1-40}$ peptide aggregation *in vitro*, and protected against Aβ-induced cytotoxicity in neuronal cells. Furthermore, the complexes differentiated between the aggregated and unaggregated forms of $A\beta_{1-40}$ peptide on the basis of their emission response.

Over the past few years, vast efforts have been dedicated to the development of imaging probes and inhibitors for the diagnosis and treatment of Alzheimer's disease, which is a highly common neurodegenerative disorder characterized by the progressive loss of cognitive ability[1,2]. One of the strategies for the treatment of Alzheimer's disease is the development of inhibitors that prevent the misfolding and self-assembling aggregation of monomeric Aβ peptides into neurotoxic fibrils[1]. Many inhibitors have been reported to inhibit Aβ peptide aggregation[3–6], such as short peptides[7,8], organic molecules[9–16], supramolecular cucurbit[7]uril[17], polyoxometalates[18,19], nanoparticles[20] and ligand-functionalized quantum dots[21]. Meanwhile, the development of new diagnostic probes for Aβ fibrillation has also been an important goal. The early diagnosis of Alzheimer's disease may allow for palliative treatment to alleviate symptoms or to slow down the progression of the disease. A number of luminescent probes have been developed for the specific labeling and imaging of Aβ plaques, such as luminescent conjugated polythiophenes[22] and common fluorescent dyes[23–31]. Dual-role imaging agents and aggregation inhibitors of Aβ may serve a bifunctional purpose for Alzheimer's disease, as the inhibition of Aβ fibrillogenesis may be monitored without the need for an extraneous labeling agent. However, to our knowledge, only a few examples of dual-function inhibitors and probes of Aβ have been reported in recent years. Organic dyes commonly used for labeling Aβ fibrils, including Congo Red and Thioflavine T (ThT), have been shown to inhibit Aβ aggregation at high concentrations of dyes[32].

Luminescent transition metal complexes have found emerging use for the design of chemical and biological sensors[33,34] in view of their useful photophysical properties, such as tunable excitation and emission wavelengths (from blue to red), high luminescent quantum yields, and relatively long phosphorescent lifetimes[33]. At the same time, transition metal complexes have been increasingly regarded as a promising alternative to organic compounds as therapeutic agents for the treatment of human diseases[35–41]. Due to the well-defined three-dimensional structure of transition metal complexes, highly specific interactions between metal complexes and biomolecules can be obtained through modification of the steric and electronic nature of the organic ligands surrounding the metal centre. In the context of Alzheimer's disease, metal complexes such as Pt(II)[42–48], binuclear Ru(II)–Pt(II)[49], Ru(II)[50–52], Co(III)[53] and Ir(III) or Rh(III) solvato[54] complexes have been reported to inhibit the aggregation of Aβ peptide[55–57]. Furthermore, luminescent metal complexes such as Ru(II)[58,59], Re(I)[60] complexes have also

[1]Department of Chemistry, Hong Kong Baptist University, Kowloon Tong, Hong Kong, China. [2]State Key Laboratory of Quality Research in Chinese Medicine, Institute of Chinese Medical Sciences, University of Macau, Macao, China. *These authors contributed equally to this work. Correspondence and requests for materials should be addressed to H.-W.L. (email: hwli@hkbu.edu.hk) or C.-H.L. (email: duncanleung@umac.mo) or D.-L.M. (email: edmondma@hkbu.edu.hk)

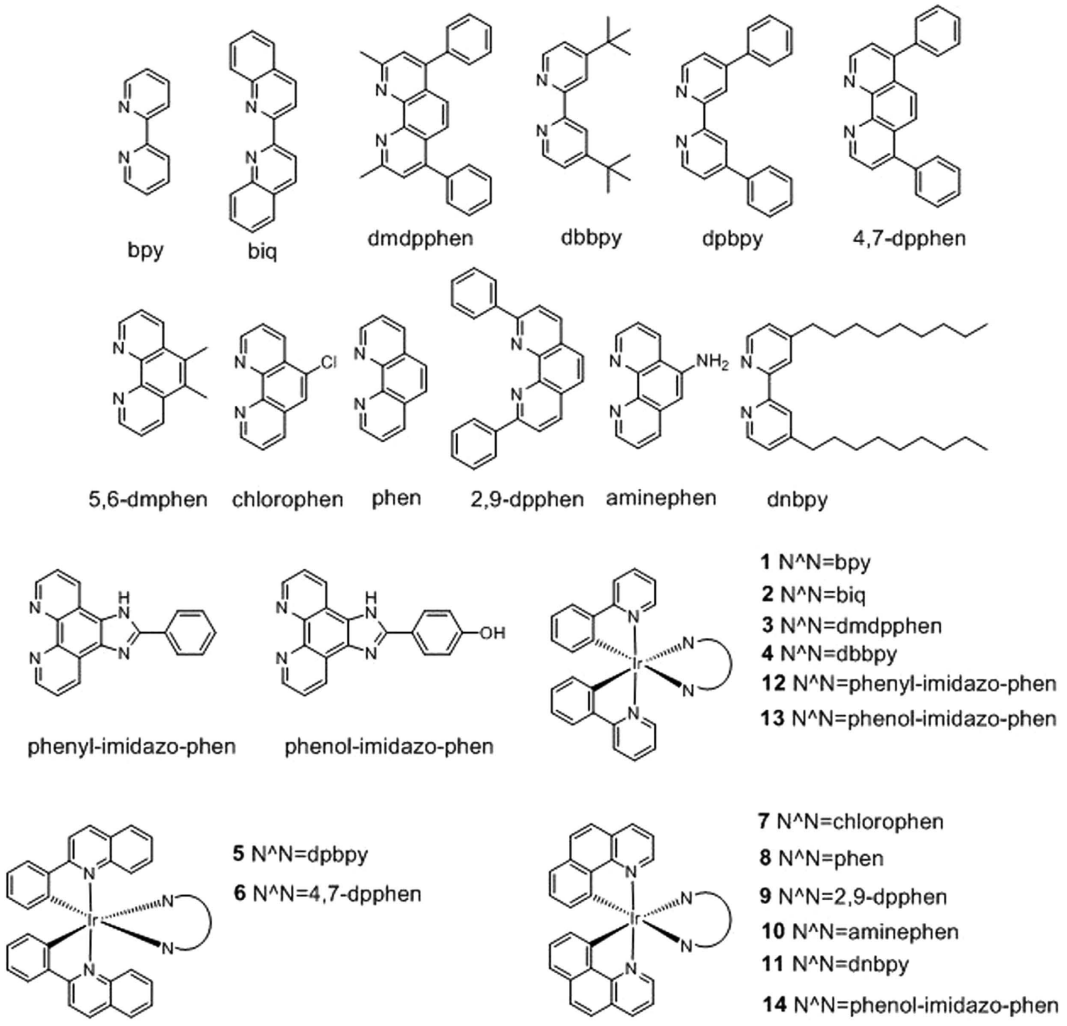

Figure 1. Chemical structures of the luminescent Ir(III) complexes 1–14 which were synthesized and evaluated in this study.

been used to monitor the Aβ fibrillation process[30,55]. However, few transition metal complexes have been reported to be dual inhibitors and luminescent probes of Aβ. Moreover, while iridium(III) complexes have been widely used as probes for various biomolecules, their application as dual inhibitors and probes of beta-amyloid fibrillogenesis has not been previously described.

Our group has previously reported the application of Ir(III) and Rh(III) solvato complexes as inhibitors of amyloid fibrillogenesis and as luminescent probes for Aβ peptide[54]. Mass spectrometry experiments indicated that the Rh(III) solvato complex formed 1:1 covalent adducts with $A\beta_{1-40}$, presumably through coordination of the N-donor histidine residue of $A\beta_{1-40}$ to the Rh(III) center via displacement of the aqua ligands. Encouraged by our previous results with Group 9 solvato compounds, we sought to investigate the ability of kinetically inert Ir(III) complexes to function as dual imaging agents and inhibitors of Aβ peptide aggregation. We report herein the synthesis of a series of luminescent Ir(III) complexes containing various C^N and N^N ligands, and their ability to detect and inhibit Aβ fibrillation. We envisage that these kinetically inert Ir(III) complexes may be developed as a novel class of dual-purpose probes and inhibitors of Aβ aggregation for the effective diagnosis and/or treatment of Alzheimer's disease.

Results

A library of twelve luminescent Ir(III) complexes (**1**–**12**, Fig. 1) were initially examined for their ability to interact with different forms of $A\beta_{1-40}$ by emission titration. Of these twelve complexes, **12** bearing the 2-phenyl-1H-imidazo[4, 5-*f*][1,10]phenanthroline (phenyl-imidazo-phen) N^N ligand displayed the $I_{fibril}/I_{monomer}$ ratio (>1.5), indicating that it possessed the highest distinguishing ability for detecting $A\beta_{1-40}$ fibrils over $A\beta_{1-40}$ monomers (Figure S1). However, **1**–**11** were unable to effectively discriminate

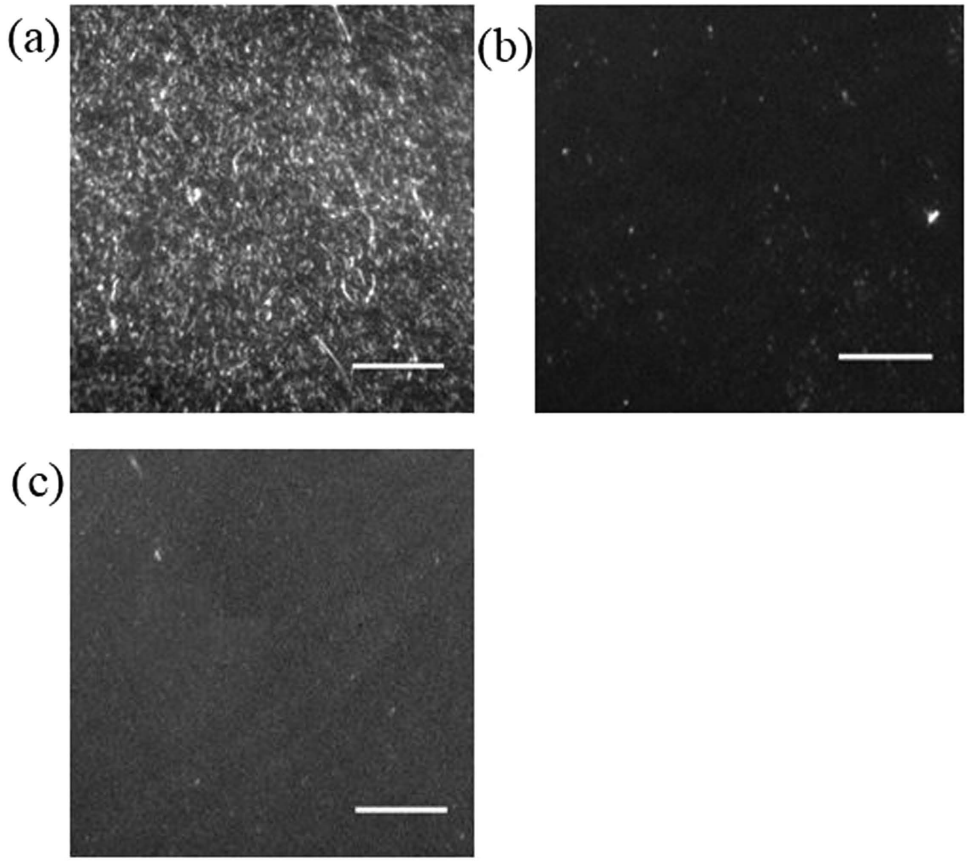

Figure 2. Inhibition of seed-mediated $A\beta_{1-40}$ fibril growth by Ir(III) complexes. TIRFM images of $A\beta_{1-40}$ fibrils grown in the (**a**) absence and presence of (**b**) **13**, (**c**) **14** after incubation at 37 °C for 1 h. The scale bar for TIRFM is 20 μm.

between $A\beta_{1-40}$ monomers and fibrils. Based on the structure of **12**, we designed and synthesized **13** and **14**. The characterization and photophysical properties of **1**–**14** are given in the ESI (Table S1).

Complexes **12**–**14** were investigated for their ability to inhibit the fibrillogenesis of $A\beta_{1-40}$. Given that these complexes could detect $A\beta_{1-40}$ fibrils over $A\beta_{1-40}$ monomers, the kinetics of $A\beta_{1-40}$ aggregation in the presence of the complexes could be monitored without the need for an external labeling agent. The results revealed typical sigmoidal growth curves in seed-mediated Aβ fibrillation when $A\beta_{1-40}$ monomers was incubated with ThT or **12**–**14** (Figure S2a and S2b). However, fibrillogenesis was partial retarded by **13** and completely inhibited by **14**, indicating that these two complexes were able to inhibit $A\beta_{1-40}$ peptide aggregation. As both **13** and **14** contain the phenol-imidazo-phen N^N ligand, the effect of that ligand alone on $A\beta_{1-40}$ peptide aggregation was investigated. The results showed that the presence of the N^N ligand alone had no inhibitory effect on $A\beta_{1-40}$ peptide aggregation, highlighting the importance of the iridium(III) metal center in maintaining the octahedral structure of the active complexes (Figure S2c). Moreover, total internal reflection fluorescence microscopy (TIRFM) with laser excitation was used to observe the ThT-labelled fibrils with high sensitivity. In the absence of Ir(III) complexes, the fluorescence images of the $A\beta_{1-40}$ peptides incubated by the seed-mediated method showed dense spots, corresponding to newly genereted $A\beta_{1-40}$ fibrils (Fig. 2a). In contrast, these spots partially or completely disappeared when the samples were treated with **13** (Fig. 2b) or **14** (Fig. 2c), indicating that **13** and **14** could partially or completely inhibit the fibrillogenesis of amyloid peptides, respectively. Transmission electron microscopy (TEM) images further confirmed the ability of the Ir(III) complexes to inhibit seed-mediated Aβ aggregation. In the control experiment (Fig. 3a), $A\beta_{1-40}$ grewinto thick, dense and long hair-like fibrils. However, when the sample was incubated with **13,** the TEM image showed short flake-like fibris (Fig. 3b), indicating that **13** was able to partially inhibit the $A\beta_{1-40}$ aggregation. Furthermore, incubation of the sample with **14** resulted in the complete absence of elongated fibrils, and only the preformed fibril seeds were observed (Fig. 3c), indicating the complete inhibition amyloid fibrillogenesis by **14**. Moreover, the fibrillogenesis kinetics of $A\beta_{1-40}$ in the presence of various concentrations of **14** showed that the inhibition of $A\beta_{1-40}$ aggregation by **14** was concentration-dependent (Figure S3). At 50 μM of **14**, the inhibition of 25 μM of $A\beta_{1-40}$ peptides was nearly completely inhibited.

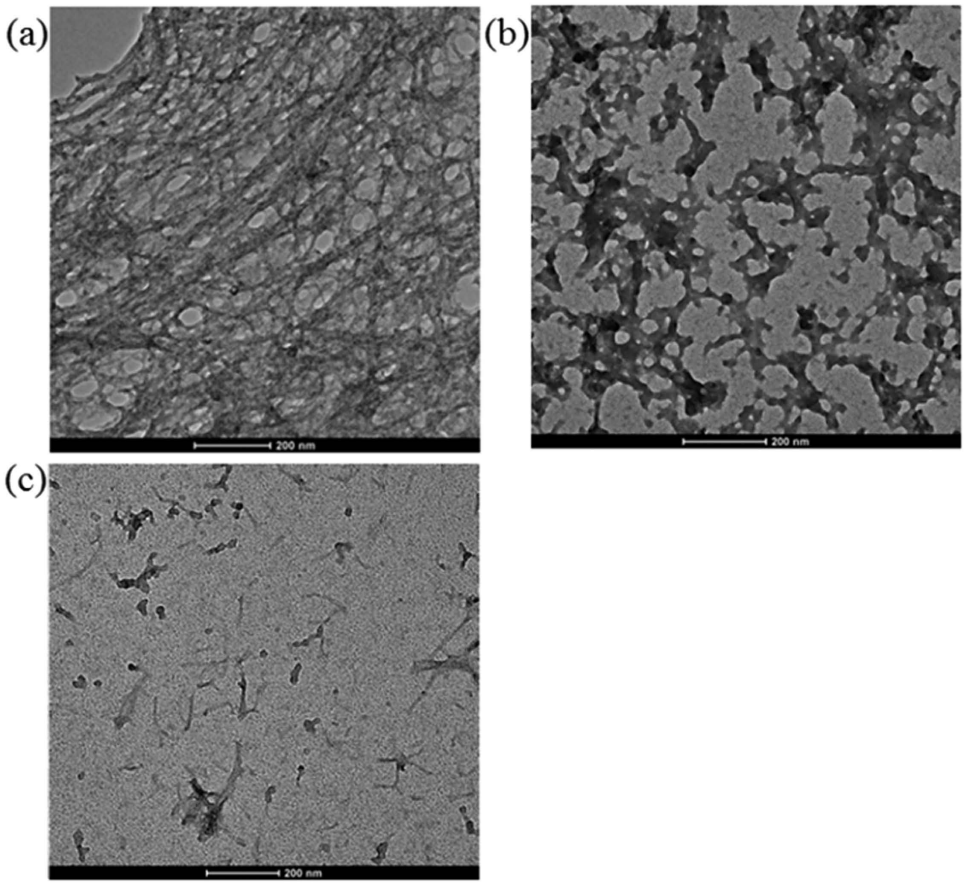

Figure 3. Inhibition of seed-mediated $A\beta_{1-40}$ fibril growth by Ir(III) complexes. TEM images of $A\beta_{1-40}$ fibrils grown in the (**a**) absence and presence of (**b**) **13**, (**c**) **14** after incubation at 37 °C for 1 h. The scale bar for TEM is 200 nm.

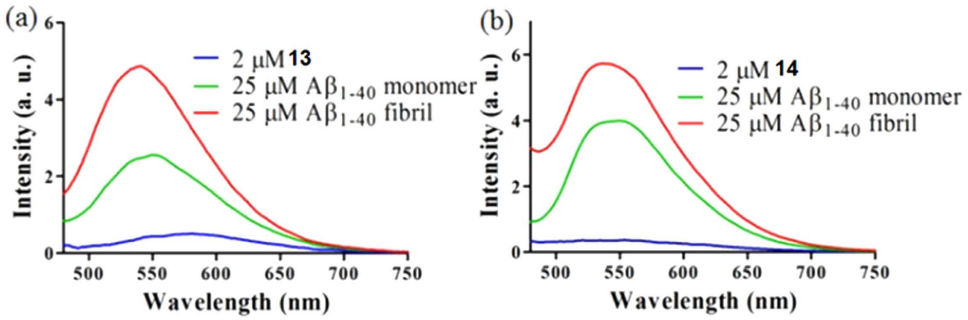

Figure 4. Luminescence response of 2 μM of (a) 13 and (b) 14 in the absence or presence of 25 μM $A\beta_{1-40}$ monomers or fibrils. $\lambda_{Ex} = 360$ nm.

Encouraged by the promising activity of **13** and **14** against Aβ aggregation, we investigated that the luminescence behaviour of **13** and **14** towards different forms of $A\beta_{1-40}$. The results showed that both complexes displayed a significantly enhanced luminescence response in the presence of the $A\beta_{1-40}$ monomers or fibrils (Fig. 4). **13** exhibited *ca.* 6- and 12-fold emission enhancements at $\lambda_{max} = 540$ nm in the presence of comparable mass concentrations of $A\beta_{1-40}$ monomers and fibrils, respectively. On the other hand, **14** showed *ca.* 11- and 18-fold emission enhancements at $\lambda_{max} = 540$ nm in the presence of $A\beta_{1-40}$ monomers and fibrils. Taken together, these two Ir(III) complexes showed luminescence enhancement to the presence of $A\beta_{1-40}$ monomers and fibrils to different extents. We presume that this behaviour of the Ir(III) complexes towards the $A\beta_{1-40}$ peptide may be due to the ability of the complexes to bind to a hydrophobic region within the peptide, thus protecting the complexes from non-radiative decay by solvent quenching and thereby giving rise to an enhanced luminescence response. The differential

luminescence response of the complexes towards $A\beta_{1-40}$ monomers and fibrils may be due to the different microenvironments experienced by the Ir(III) complexes upon binding to the $A\beta_{1-40}$ monomers or the fibrils.

ESI-TOF mass spectrometry experiments were performed to examine the binding of the Ir(III) complexes to $A\beta_{1-40}$ peptide. The mass spectrum of the $A\beta_{1-40}$ monomer in the absence of the Ir(III) complexes shows two characteristic peaks at 1083 and 1444, corresponding to the 4+ and 3+ ionization states of the $A\beta_{1-40}$ monomer, respectively (Figure S4a). However, incubation of the $A\beta_{1-40}$ peptide with **13** (Figure S4b) or **14** (Figure S4c) produced no new peaks in the mass spectra besides those corresponding to the free complex (813 for **13** and 861 for **14**), suggesting that the Ir(III) complexes were not covalently bound to the $A\beta_{1-40}$ peptide.

The cytotoxicity of the most potent Ir(III) complex **14** was examined using the 3-(4,5-dime thylthiazol-2-yl)-2,5-diphenyltetrazolium bromide (MTT) assay (Figure S5). Neuroblastoma cells (SH-SY5Y) were incubated in the presence of different concentrations for 24 h and cell viability was examined using the MTT assay. The IC_{50} value of **14** was estimated to be $>100\,\mu M$ at 24 h of exposure. Notably, these IC_{50} values are significantly higher than the concentration of **14** required for complete inhibition of $A\beta_{1-40}$ peptide aggregation, suggesting the presence of a therapeutic window whereby $A\beta_{1-40}$ peptide aggregation can be controlled without significant damage to brain cells.

The effect of **14** on $A\beta_{1-40}$-induced cytotoxicity in SH-SY5Y cells and mouse primary cortical cells was also investigated. The cytotoxicity of three different forms of $A\beta_{1-40}$ peptide in the presence and the absence of **14** were examined: $A\beta_{1-40}$ peptide monomer (M), $A\beta_{1-40}$ peptide monomer with seeded fibrils (MS) and $A\beta_{1-40}$ fibril (F) (Fig. 5). The results showed that treatment of cells with different forms of $A\beta_{1-40}$ peptides caused toxicity to SH-SY5Y cells and mouse primary cortical cells (Fig. 4a,c,e,g). Encouragingly, **14** exhibited a neuroprotective effect against the cytotoxicity induced by all three forms of $A\beta_{1-40}$ peptide at $[A\beta_{1-40}]/[\mathbf{14}]$ ratios of 0.2, 1.0, or 5.0 for SH-SY5Y cells (Fig. 5a,b) or mouse primary cortical cells (Fig. 5e,f) after 2 h of incubation. The neuroprotective effects of **14** were still observable after 24 h of incubation of **14** (Fig. 5c,d,g,h). As a negative control, we also investigated the effect of **12**, which showed no effect against amyloid aggregation, on $A\beta_{1-40}$-induced toxicity. The results showed that **12** had no neuroprotective effect against cytotoxicity induced by all three forms of $A\beta_{1-40}$ peptide at $[A\beta_{1-40}]/[\mathbf{12}]$ ratios of 0.2, 1.0, or 5.0 in SH-SY5Y cells (Figure S6). Taken together, these data indicate that **14** displays neuroprotective effects against Aβ-mediated cytotoxicity when administered at a low enough dosage in SH-SY5Y cells and mouse primary cortical cells.

Discussion

In conclusion, a library of 12 luminescent Ir(III) complexes containing various C^N and N^N ligands were initially screened as luminescent probes for $A\beta_{1-40}$ peptide. Based on the ability of **12** for distinguishing $A\beta_{1-40}$ fibrils over monomers, **13** and **14** were further synthesized and tested. The novel Ir(III) complex **14** emerged as the most potent candidate and was shown to inhibit $A\beta_{1-40}$ peptide aggregation as revealed by a luminescence assay, as well as TIRFM and TEM imaging. Notably, $A\beta_{1-40}$ peptide aggregation was nearly completely inhibited at $50\,\mu M$ of **14**. A neuroprotective effect of **14** against $A\beta_{1-40}$-induced cytotoxicity in SH-SY5Y cells and mouse primary cortical cells was also demonstrated. Using ESI-TOF mass spectrometry, we also showed **14** was not covalently bound to the $A\beta_{1-40}$ peptide. Non-covalent probes may have a better safety index, lower cross-reactivity, and lower immunogenicity compared to covalently-binding molecules[61–63]. We envision that this work would open up new avenues for the development of dual-role imaging agents and aggregation inhibitors of Aβ for the treatment of Alzheimer's disease.

Methods

Chemicals and materials. Reagents, unless specified, were purchased from Sigma Aldrich (St. Louis, MO) and used as received. Iridium chloride hydrate ($IrCl_3{\cdot}xH_2O$) was purchased from Precious Metals Online (Australia).

General experiment. Mass spectrometry was performed at the Mass Spectroscopy Unit at the Department of Chemistry, Hong Kong Baptist University, Hong Kong (China). Deuterated solvents for NMR purposes were obtained from Armar and used as received.

^1H and ^{13}C NMR were recorded on a Bruker Avance 400 spectrometer operating at 400 MHz (^1H) and 100 MHz (^{13}C). ^1H and ^{13}C chemical shifts were referenced internally to solvent shift (acetone-d_6: ^1H δ 2.05, ^{13}C δ 29.8). Chemical shifts (δ are quoted in ppm, the downfield direction being defined as positive. Uncertainties in chemical shifts are typically ±0.01 ppm for ^1H and ±0.05 for ^{13}C. Coupling constants are typically ±0.1 Hz for ^1H-^1H and ±0.5 Hz for ^1H-^{13}C couplings. The following abbreviations are used for convenience in reporting the multiplicity of NMR resonances: s, singlet; d, doublet; t, triplet; m, multiplet. All NMR data was acquired and processed using standard Bruker software (Topspin).

Photophysical measurement. Emission spectra and lifetime measurements for complexes were performed as previously reported method[64].

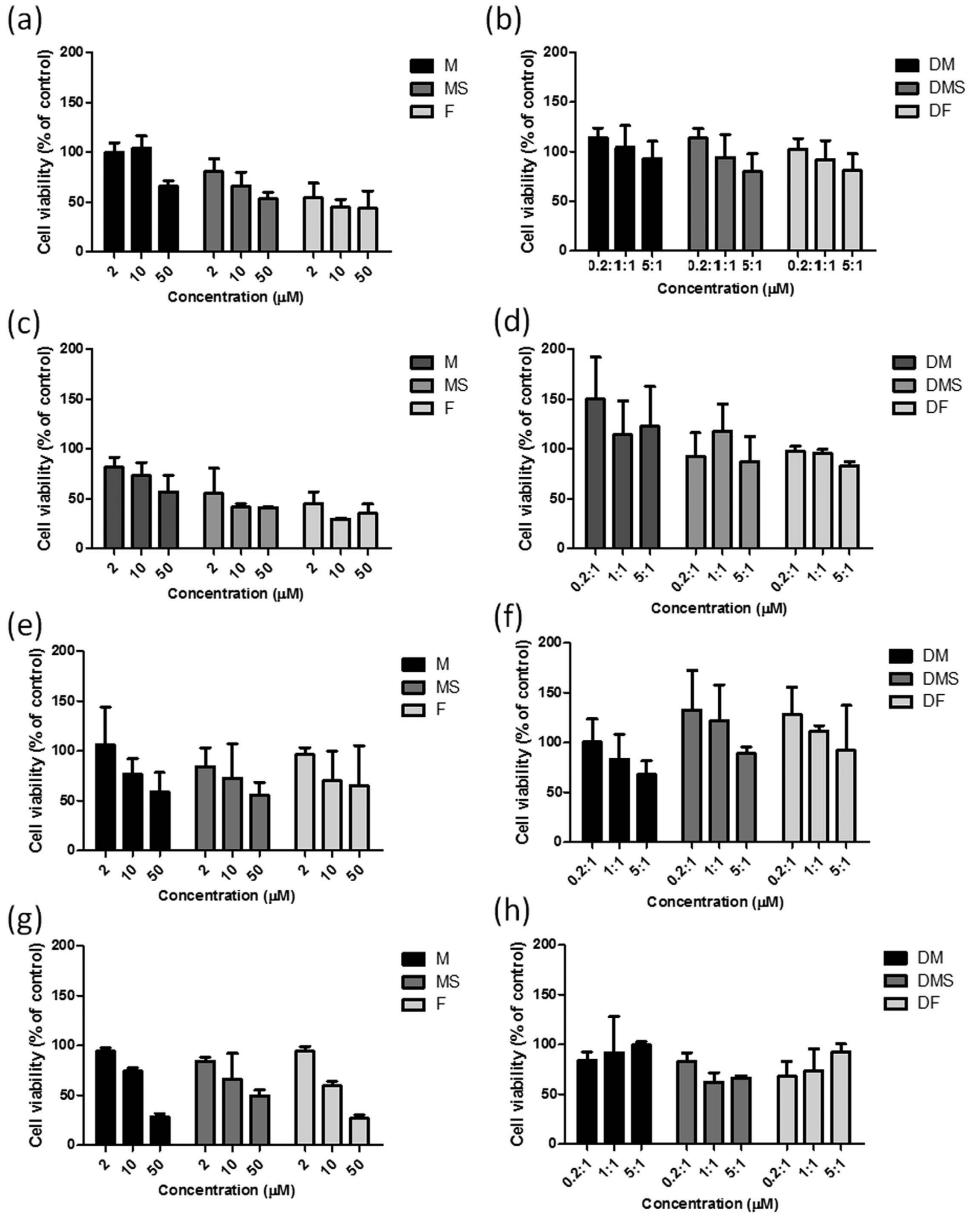

Figure 5. Neuroprotective effect of 14 against $A\beta_{1-40}$ peptide-induced cytotoxicity towards (a–d) human neuroblastoma SH-SY5Y cells and (e–h) mouse primary cortical cells. Cell viability is expressed as a percentage of control cells exposed to 0.5% DMSO. The histograms show the cell viability of various concentrations of $A\beta_{1-40}$ peptide monomer (M), $A\beta_{1-40}$ peptide with seeded fibril (MS), and fibrillar $A\beta_{1-40}$ peptide (F), in the presence of **14**. Various forms of $A\beta_{1-40}$ peptide were incubated for (**a**,**b**,**e**,**f**) 2 h, and for (**c**,**d**,**g**,**h**) 24 h at [$A\beta_{1-40}$]:[**14**] ratios of 0.2:1, 1:1, and 5:1.

Transmission electron microscopy (TEM) imaging. 8 μL of diluted sample solution was applied to a carbon-coated copper grid (T200H-Cu Electron Microscopy Sciences, Washington, USA), dried, and was then negatively stained with 2% uranyl acetate. The stained sample was then allowed to be dried. Transmission electron micrographs were recorded using a Technai G2 Transmission Electron Microscope (FEI, USA) with an acceleration voltage of 200 kV.

Total internal reflection fluorescence microscopy (TIRFM) imaging. This experimental system and operation was as previously described[52]. After the incubation period, the organic dye ThT (the mole ratio of $A\beta_{1-40}$ and ThT is 1:2) was added to label the $A\beta_{1-40}$ fibrils. Then, a 445 nm diode laser (50 mW, LQC445-40E, Newport, USA) was used for the excitation of the ThT-labeled $A\beta_{1-40}$. Images were obtained by using the WinSpec/32 software (Princeton Instruments, Version 2.5.22.0, Downingtown, PA).

Preparation of stock solution of tested Ir(III) complexes. The stock solution of all the tested Ir(III) complexes are 10 mM in DMSO.

Emission measurement in buffered solution. Ir(III) complexes (2 μM) and different concentrations of $A\beta_{1-40}$ monomer/fibril were added into phosphate buffer (50 mM Na_2HPO_4, pH 7.4). The mixtures were allowed to equilibrate at room temperature for 3 min without degassing. Emission spectra were recorded on PTI TimeMaster C720 Spectrometer.

Preparation of $A\beta_{1-40}$ fibrils for seeding. The incubation of $A\beta_{1-40}$ fibrils and seeds used the previously reported method[52].

ThT and Ir(III) complexes luminescence binding assays. 50 μM of ThT/complex solution (1%) was incubated with 25 μM $A\beta_{1-40}$ monomer solution in phosphate buffer at 37 °C. The luminescence intensity at different time points was measured on a PTI TimeMaster C720 Spectrometer.

Mass spectrometry experiments. A solution of containing **13** or **14** (25 μM, final concentration) (final DMSO concentration $\leq$1%) and $A\beta_{1-40}$ peptide monomers (50 μM, final concentration) were mixed in 1 mM ammonium acetate (pH 7.6), and injected into the ESI-TOF-MS at a rate of 3 L/min. ESI-TOF-MS experiments were conducted in the negative-ion mode with a Bruker MicrOTOFQ mass spectrometer. The capillary voltage was set at +3500 V, and the dry N_2 gas flow was 4.0 L/min at 100 °C. Data were analyzed by the software Bruker Daltonics Data Analysis.

Cell viability analysis. The cell viability analysis is referenced from a reported method[52]. Specifically, SH-SY5Y cells or primary cortical cells were plated into 96-well plates at a density of 5×10^4 cells/well in cell culture medium. At the next day, the culture medium was replaced with the same medium with 0.2% serum and containing 10 μM **12** and **14** together with monomer, mixture of monomer and seed, and seeding fibril respectively in 1-to-0.2, 1-to-1 or 1-to-5 ratio (final concentration of DMSO $\leq$ 1.6%). Cells were incubated at 37 °C for 2 and 24 h, respectively. The medium of each well was replaced with 3-(4,5-dimethylthiazol-2-yl)-2,5-diphenyltetrazolium bromide (MTT) solution (5 mg/mL) and further incubated for 3 h at 37 °C. The MTT solution was aspirated off and then 100 μL of DMSO was added to each well to dissolve the formazan crystals. The plates were agitated on a plate shaker for 15 min and the absorbance was measured at 570 nm using a SpectraMax M5 microplate reader (Molecular Devices). Wells without cells were used as blanks and were subtracted as background from each sample. Results were expressed as a percentage of control.

References

1. Hardy, J. & Selkoe, D. J. The Amyloid Hypothesis of Alzheimer's Disease: Progress and Problems on the Road to Therapeutics. *Science* **297,** 353–356 (2002).
2. Ballatore, C., Lee, V. M. Y. & Trojanowski, J. Q. Tau-mediated neurodegeneration in Alzheimer's disease and related disorders. *Nat. Rev. Neurosci.* **8,** 663–672 (2007).
3. Wang, Q., Yu, X., Li, L. & Zheng, J. Inhibition of Amyloid-β Aggregation in Alzheimer's Disease. *Curr. Pharm. Des.* **20,** 1223–1243 (2014).
4. Cheng, B. *et al.* Inhibiting toxic aggregation of amyloidogenic proteins: A therapeutic strategy for protein misfolding diseases. *Biochim. Biophys. Acta* **1830,** 4860–4871 (2013).
5. Zhang, M. *et al.* Nanomaterials for Reducing Amyloid Cytotoxicity. *Adv. Mater.* **25,** 3780–3801 (2013).
6. Belluti, F., Rampa, A., Gobbi, S. & Bisi, A. Small-molecule inhibitors/modulators of amyloid-β peptide aggregation and toxicity for the treatment of Alzheimer's disease: a patent review (2010–2012). *Expert Opin. Ther. Pat.* **23,** 581–596 (2013).
7. Yamin, G., Ruchala, P. & Teplow, D. B. A Peptide Hairpin Inhibitor of Amyloid β-Protein Oligomerization and Fibrillogenesis. *Biochemistry* **48,** 11329–11331 (2009).
8. Taylor, M. *et al.* Development of a Proteolytically Stable Retro-Inverso Peptide Inhibitor of β-Amyloid Oligomerization as a Potential Novel Treatment for Alzheimer's Disease. *Biochemistry* **49,** 3261–3272 (2010).
9. Cohen, T., Frydman-Marom, A., Rechter, M. & Gazit, E. Inhibition of Amyloid Fibril Formation and Cytotoxicity by Hydroxyindole Derivatives. *Biochemistry* **45,** 4727–4735 (2006).
10. Reinke, A. A. & Gestwicki, J. E. Structure–activity Relationships of Amyloid Beta-aggregation Inhibitors Based on Curcumin: Influence of Linker Length and Flexibility. *Chem. Biol. Drug Des.* **70,** 206–215 (2007).
11. Hong, H.-S. *et al.* Inhibition of Alzheimer's amyloid toxicity with a tricyclic pyrone molecule *in vitro* and *in vivo*. *J. Neurochem.* **108,** 1097–1108 (2009).
12. Reinke, A. A., Ung, P. M. U., Quintero, J. J., Carlson, H. A. & Gestwicki, J. E. Chemical Probes That Selectively Recognize the Earliest Aβ Oligomers in Complex Mixtures. *J. Am. Chem. Soc.* **132,** 17655–17657 (2010).
13. Mishra, R. *et al.* Small-Molecule Inhibitors of Islet Amyloid Polypeptide Fibril Formation. *Angew. Chem. Int. Ed.* **47,** 4679–4682 (2008).
14. Arai, T. *et al.* Rational Design and Identification of a Non-Peptidic Aggregation Inhibitor of Amyloid-β Based on a Pharmacophore Motif Obtained from cyclo[-Lys-Leu-Val-Phe-Phe-]. *Angew. Chem. Int. Ed.* **53,** 8236–8239 (2014).
15. Razavi, H. *et al.* Benzoxazoles as Transthyretin Amyloid Fibril Inhibitors: Synthesis, Evaluation, and Mechanism of Action. *Angew. Chem. Int. Ed.* **42,** 2758–2761 (2003).
16. Sharma, A. K. *et al.* Bifunctional Compounds for Controlling Metal-Mediated Aggregation of the Aβ42 Peptide. *J. Am. Chem. Soc.* **134,** 6625–6636 (2012).
17. Lee, H. H. *et al.* Supramolecular Inhibition of Amyloid Fibrillation by Cucurbit[7]uril. *Angew. Chem. Int. Ed.* **53,** 7461–7465 (2014).
18. Geng, J., Li, M., Ren, J., Wang, E. & Qu, X. Polyoxometalates as Inhibitors of the Aggregation of Amyloid β Peptides Associated with Alzheimer's Disease. *Angew. Chem. Int. Ed.* **50,** 4184–4188 (2011).

19. Gao, N. *et al.* Transition-metal-substituted polyoxometalate derivatives as functional anti-amyloid agents for Alzheimer's disease. *Nat. Commun.* **5,** 3422 (2014).
20. Yoo, S. I. *et al.* Inhibition of Amyloid Peptide Fibrillation by Inorganic Nanoparticles: Functional Similarities with Proteins. *Angew. Chem. Int. Ed.* **50,** 5110–5115 (2011).
21. Xiao, L., Zhao, D., Chan, W.-H., Choi, M. M. F. & Li, H.-W. Inhibition of beta 1–40 amyloid fibrillation with N-acetyl-l-cysteine capped quantum dots. *Biomaterials* **31,** 91–98 (2010).
22. Herland, A., Thomsson, D., Mirzov, O., Scheblykin, I. G. & Inganas, O. Decoration of amyloid fibrils with luminescent conjugated polymers. *J. Mater. Chem.* **18,** 126–132 (2008).
23. Nesterov, E. E. *et al. In Vivo* Optical Imaging of Amyloid Aggregates in Brain: Design of Fluorescent Markers. *Angew. Chem. Int. Ed.* **44,** 5452–5456 (2005).
24. Chang, W. M. *et al.* ANCA: A Family of Fluorescent Probes that Bind and Stain Amyloid Plaques in Human Tissue. *ACS Chem. Neurosci.* **2,** 249–255 (2011).
25. Li, M. *et al. In Situ* Monitoring Alzheimer's Disease β-Amyloid Aggregation and Screening of Aβ Inhibitors Using a Perylene Probe. *Small* **9,** 52–55 (2013).
26. Mishra, R., Sjolander, D. & Hammarstrom, P. Spectroscopic characterization of diverse amyloid fibrils *in vitro* by the fluorescent dye Nile red. *Mol. Biosyst.* **7,** 1232–1240 (2011).
27. Hong, Y. *et al.* Monitoring and Inhibition of Insulin Fibrillation by a Small Organic Fluorogen with Aggregation-Induced Emission Characteristics. *J. Am. Chem. Soc.* **134,** 1680–1689 (2011).
28. Cui, M. *et al.* Smart Near-Infrared Fluorescence Probes with Donor–Acceptor Structure for *in Vivo* Detection of β-Amyloid Deposits. *J. Am. Chem. Soc.* **136,** 3388–3394 (2014).
29. Wolfe, L. S. *et al.* Protein-induced photophysical changes to the amyloid indicator dye thioflavin T. *Proc. Natl. Acad. Sci. USA* **107,** 16863–16868 (2010).
30. Ma, D.-L. *et al.* Current Advancements in Aβ Luminescent Probes and Inhibitors of Aβ Aggregation. *Curr. Alzheimer Res.* **9,** 830–843 (2012).
31. Nilsson, K. P. R. Small organic probes as amyloid specific ligands – Past and recent molecular scaffolds. *FEBS Lett.* **583,** 2593–2599 (2009).
32. Lorenzo, A. & Yankner, B. A. Beta-amyloid neurotoxicity requires fibril formation and is inhibited by congo red. *Proc. Natl. Acad. Sci. USA* **91,** 12243–12247 (1994).
33. Zhao, Q., Huang, C. & Li, F. Phosphorescent heavy-metal complexes for bioimaging. *Chem. Soc. Rev.* **40,** 2508–2524 (2011).
34. Zhao, Q., Li, F. & Huang, C. Phosphorescent chemosensors based on heavy-metal complexes. *Chem. Soc. Rev.* **39,** 3007–3030 (2010).
35. Meggers, E. Exploring biologically relevant chemical space with metal complexes. *Curr. Opin. Chem. Biol.* **11,** 287–292 (2007).
36. Meggers, E. Targeting proteins with metal complexes. *Chem. Commun.* 1001–1010, doi: 10.1039/b813568a (2009).
37. Meggers, E. From Conventional to Unusual Enzyme Inhibitor Scaffolds: The Quest for Target Specificity. *Angew. Chem. Int. Ed.* **50,** 2442–2448 (2011).
38. Gasser, G., Ott, I. & Metzler-Nolte, N. Organometallic Anticancer Compounds. *J. Med. Chem.* **54,** 3–25 (2010).
39. Ott, I. & Gust, R. Non Platinum Metal Complexes as Anti-cancer Drugs. *Archiv. der. Pharmazie*. **340,** 117–126 (2007).
40. Wong, C.-Y., Chung, L.-H., Lu, L., Wang, M., He, B., Liu, L.-J., Leung, C.-H., & Ma, D.-L. Dual inhibition and monitoring of beta-amyloid fibrillation by a luminescent iridium(III) complex. *Curr. Alzheimer Res.* **12,** 439–443 (2015).
41. Chan, S.L.-F., Lu, L., Lam, T.-L., Yan, S.-C., Leung, C.-H., & Ma, D.-L. A novel tetradentate ruthenium(II) complex containing tris(2-pyridylmethyl)amine (tpa) as an inhibitor of beta-amyloid fibrillation. *Curr. Alzheimer Res.* **12,** 434–438 (2015).
42. Barnham, K. J. *et al.* Platinum-based inhibitors of amyloid-β as therapeutic agents for Alzheimer's disease. *Proc. Natl. Acad. Sci. USA* **105,** 6813–6818 (2008).
43. Kenche, V. B. *et al.* Development of a Platinum Complex as an anti-Amyloid Agent for the Therapy of Alzheimer's Disease. *Angew. Chem. Int. Ed.* **52,** 3374–3378 (2013).
44. Ma, G. *et al.* Identification of [$PtCl_2$(phen)] Binding Modes in Amyloid-β Peptide and the Mechanism of Aggregation Inhibition. *Chem. Eur. J.* **17,** 11657–11666 (2011).
45. Ma, G. *et al.* PtCl2(phen) disrupts the metal ions binding to amyloid-β peptide. *Metallomics* **5,** 879–887 (2013).
46. Streltsov, V. A. *et al.* Structural insights into the interaction of platinum-based inhibitors with the Alzheimer's disease amyloid-β peptide. *Chem. Commun.* **49,** 11364–11366 (2013).
47. Wang, X., Wang, X., Zhang, C., Jiao, Y. & Guo, Z. Inhibitory action of macrocyclic platiniferous chelators on metal-induced Aβ aggregation. *Chem. Sci.* **3,** 1304–1312 (2012).
48. Collin, F., Sasaki, I., Eury, H., Faller, P. & Hureau, C. Pt(II) compounds interplay with Cu(II) and Zn(II) coordination to the amyloid-β peptide has metal specific consequences on deleterious processes associated to Alzheimer's disease. *Chem. Commun.* **49,** 2130–2132 (2013).
49. Kumar, A. *et al.* Inhibition of Aβ42 Peptide Aggregation by a Binuclear Ruthenium(II)−Platinum(II) Complex: Potential for Multimetal Organometallics as Anti-amyloid Agents. *ACS Chem. Neurosci.* **1,** 691–701 (2010).
50. Vyas, N. A. *et al.* Ruthenium(II) polypyridyl complex as inhibitor of acetylcholinesterase and Aβ aggregation. *Eur. J. Med. Chem.* **75,** 375–381 (2014).
51. Valensin, D. *et al. fac*-$[Ru(CO)_3]^{2+}$ Selectively Targets the Histidine Residues of the β-Amyloid Peptide 1-28. Implications for New Alzheimer's Disease Treatments Based on Ruthenium Complexes. *Inorg. Chem.* **49,** 4720–4722 (2010).
52. Messori, L., Camarri, M., Ferraro, T., Gabbiani, C. & Franceschini, D. Promising *in Vitro* anti-Alzheimer Properties for a Ruthenium(III) Complex. *ACS Med. Chem. Lett*. **4,** 329–332 (2013).
53. Heffern, M. C. *et al.* Modulation of Amyloid-β Aggregation by Histidine-Coordinating Cobalt(III) Schiff Base Complexes. *ChemBioChem* **15,** 1584–1589 (2014).
54. Man, B. Y.-W. *et al.* Group 9 metal-based inhibitors of β-amyloid (1-40) fibrillation as potential therapeutic agents for Alzheimer's disease. *Chem. Sci*. **2,** 917–921 (2011).
55. Hayne, D. J., Lim, S. & Donnelly, P. S. Metal complexes designed to bind to amyloid-β for the diagnosis and treatment of Alzheimer's disease. *Chem. Soc. Rev.* **43,** 6701–6715 (2014).
56. Valensin, D., Gabbiani, C. & Messori, L. Metal compounds as inhibitors of β-amyloid aggregation. Perspectives for an innovative metallotherapeutics on Alzheimer's disease. *Coord. Chem. Rev.* **256,** 2357–2366 (2012).
57. Li, M. *et al.* Chiral metallo-helical complexes enantioselectively target amyloid β for treating Alzheimer's disease. *J. Am. Chem. Soc.* **136,** 11655–11663 (2014).
58. Cook, N. P., Torres, V., Jain, D. & Martí, A. A. Sensing Amyloid-β Aggregation Using Luminescent Dipyridophenazine Ruthenium(II) Complexes. *J. Am. Chem. Soc.* **133,** 11121–11123 (2011).
59. Cook, N. P., Ozbil, M., Katsampes, C., Prabhakar, R. & Martí, A. A. Unraveling the Photoluminescence Response of Light-Switching Ruthenium(II) Complexes Bound to Amyloid-β. *J. Am. Chem. Soc.* **135,** 10810–10816 (2013).
60. Sathish, V. *et al.* Alkoxy bridged binuclear rhenium(I) complexes as a potential sensor for β-amyloid aggregation. *Talanta* **130,** 274–279 (2014).

61. Singh, J., Petter, R. C., Baillie, T. A. & Whitty, A. The resurgence of covalent drugs. *Nat. Rev. Drug. Discov.* **10,** 307–317 (2011).
62. Beck, P., Dubiella, C. & Groll, M. Covalent and non-covalent reversible proteasome inhibition. *Biol. Chem.* **393,** 1101–1120 (2012).
63. Patonay, G., Salon, J., Sowell, J. & Strekowski, L. Noncovalent labeling of biomolecules with red and near-infrared dyes. *Molecules* **9,** 40–49 (2004).
64. Lu, L., Chan, D.S.-H., Kwong, D.W., He, H.-Z., Leung, C.-H. & Ma, D.-L. Detection of nicking endonuclease activity using a G-quadruplex-selective luminescent switch-on probe. *Chem. Sci.* **5,** 4561–4568 (2014).

Acknowledgements

This work is supported by Hong Kong Baptist University (FRG2/14-15/004), the Health and Medical Research Fund (HMRF/13121482 and HMRF/14130522), the Research Grants Council (HKBU/201811, HKBU/204612 and HKBU/201913), the French National Research Agency/Research Grants Council Joint Research Scheme (A-HKBU201/12), State Key Laboratory of Environmental and Biological Analysis Research Grant (SKLP-14-15-P001), National Natural Science Foundation of China (21575121), Guangdong Province Natural Science Foundation (2015A030313816), Hong Kong Baptist University Century Club Sponsorship Scheme 2015, Interdisciplinary Research Matching Scheme (RC-IRMS/14-15/06), the State Key Laboratory of Synthetic Chemistry, the Science and Technology Development Fund, Macao SAR (103/2012/A3 and 098/2014/A2) and the University of Macau (MYRG091(Y3-L2)-ICMS12-LCH, MYRG2015-00137-ICMS-QRCM and MRG023/LCH/2013/ICMS).

Author Contributions

L.L., H.-J.Z., M.W. and S.-L.H. carried out all the experiments, performed the data analysis and wrote the manuscript. H.-W.L., C.-H.L. and D.-L.M. designed the experiments and analyzed the results.

Additional Information

Supplementary information accompanies this paper at http://www.nature.com/srep

Competing financial interests: The authors declare no competing financial interests.

How to cite this article: Lu, L. *et al.* Inhibition of Beta-Amyloid Fibrillation by Luminescent Iridium(III) Complex Probes. *Sci. Rep.* **5**, 14619; doi: 10.1038/srep14619 (2015).